Unambiguous Structure Characterization of a DNA−RNA Triple Helix by ^{15}N- and ^{13}C-Filtered NOESY Spectroscopy†

Maria J. P. van Dongen,‡ Hans A. Heus,‡ Sybren S. Wymenga,‡ Gijs A. van der Marel,§ Jacques H. van Boom,§ and Cornelis W. Hilbers*,‡

NSR Centre for Molecular Structure, Design, and Synthesis, Laboratory of Biophysical Chemistry, University of Nijmegen, Toernooiveld, 6525 ED Nijmegen, The Netherlands, and Gorlaeus Laboratories, Department of Organic Chemistry, State University of Leiden, P.O. Box 9502, 2300 RA Leiden, The Netherlands

Received August 22, 1995; Revised Manuscript Received November 6, 1995⊗

ABSTRACT: DNA·DNA*RNA triple helices of the pyrimidine·purine*pyrimidine motif (where · indicates Watson−Crick pairing and * indicates Hoogsteen pairing) appear to be very stable, which has important implications for the development of novel antisense strategies. Here we present the first structural NMR studies on such a system, composed of a DNA hairpin with a homopurine−homopyrimidine stem sequence and a single-stranded RNA oligonucleotide containing exclusively pyrimidine residues. In these investigations an unlabeled DNA hairpin and a uniformly ^{13}C/^{15}N-enriched RNA oligonucleotide were utilized in combination with X-edited ^{1}H NMR spectroscopy. Improved ^{15}N (ω_2) filtered NOESY and ^{13}C (ω_1) filtered NOESY are presented by which we were able to differentiate between intrastrand, i.e., DNA−DNA and RNA−RNA, and interstrand, i.e., DNA−RNA, NOE contacts. It is unambiguously established that the complex forms a right-handed triple helix, with the RNA strand situated in the major groove of the Watson−Crick stem of the hairpin. The interaction is stabilized by the formation of Hoogsteen-type base pairs between the RNA strand and the purine strand of the DNA. These strands run parallel to each other. The characterization of the DNA−RNA triple helix structure described here shows that this type of experiment forms a valuable instrument in the structure determination of bimolecular systems of nucleic acids.

Triple helices are generally thought to play an important role in various cellular processes *in vivo* (Burkholder et al., 1988, 1991; Lee et al., 1989; Ulrich et al., 1992; Hampel et al., 1994). Moreover, they are considered to form a new and potentially useful concept in nucleic acid recognition (François et al., 1989; Horne & Dervan, 1990; Pvosic & Dervan, 1990; Skoog & Maher, 1993; Ing et al., 1993; Roy, 1993). This triggered a number of research groups to elucidate the three-dimensional conformation of this structural motif. Up to now, structures of intramolecular triple helices formed by a single DNA strand accommodating different types of base triples have been published (Macaya et al., 1992; Radhakrishan & Patel, 1993, 1994a,b).

Recently, a number of reports on the effect of strand composition on triple helix stability appeared (Roberts & Crothers, 1992; Han & Dervan, 1993; Escudé et al., 1993). Although the results of these studies are not completely comparable in every detail, all of them share the general conclusion that very stable structures are obtained for pyrimidine·purine*pyrimidine-type triple helices in which the two Watson−Crick paired strands are composed of DNA and the third strand is composed of RNA. This kind of system is of great interest especially because of its role in the antisense approach, in which a target mRNA strand is inhibited by the binding of a synthetic oligonucleotide. Here we report on the first NMR[1] studies of such a complex, i.e., a DNA hairpin with a stem to which an RNA oligonucleotide is bound (Figure 1).

For the characterization of unusual nucleic acid structures like triple helices by NMR, the resonance assignments of the imino and amino protons and the subsequent analysis of their NOE contacts are crucial. For instance, NOEs between the imino protons of the pyrimidines in the third strand and the H8 protons in the purine strand, as well as cross-strand amino−amino proton NOEs between the amino protons of Hoogsteen-bound protonated cytosines and the amino protons of the Watson−Crick paired cytosines, are necessary to define the geometry of pyr·pur*pyr type base triples (see bottom part of Figure 1) (Rajagopal & Feigon, 1989; de los Santos et al., 1989; Sklenář & Feigon, 1990; Mooren et al., 1990). The interpretation of the NOE data is severely hampered, however, in the case of overlap in the exchangeable proton spectrum, as well as by the general difficulty that it is impossible to unambigiously distinguish cross-strand NOEs from those arising from intrastrand contacts. One possible way to deal with these complications is to use a structural model, derived from, e.g., X-ray data, as a starting point for the assignments. This is the approach that has been applied to the DNA triple helices studied so far and has

† This work was supported by the Dutch Foundation for Chemical Research (SON) with financial aid from the Netherlands Organization for the Advancement of Research (NWO). H.A.H. is supported by a grant from the Royal Netherlands Academy of Arts and Sciences.

* Author to whom correspondence should be addressed.
‡ University of Nijmegen.
§ University of Leiden.

⊗ Abstract published in *Advance ACS Abstracts,* January 15, 1996.

[1] Abbreviations: NMR, nuclear magnetic resonance; NOE, nuclear Overhauser enhancement; NOESY, NOE spectroscopy; OD, optical density units; GARP, globally optimized alternating phase rectangular pulse; 2D, two dimensional; HMQC, heteronuclear multiple-quantum coherence; TPPI, time-proportional phase incrementation; ppm, parts per million.

0006-2960/96/0435-1733$12.00/0

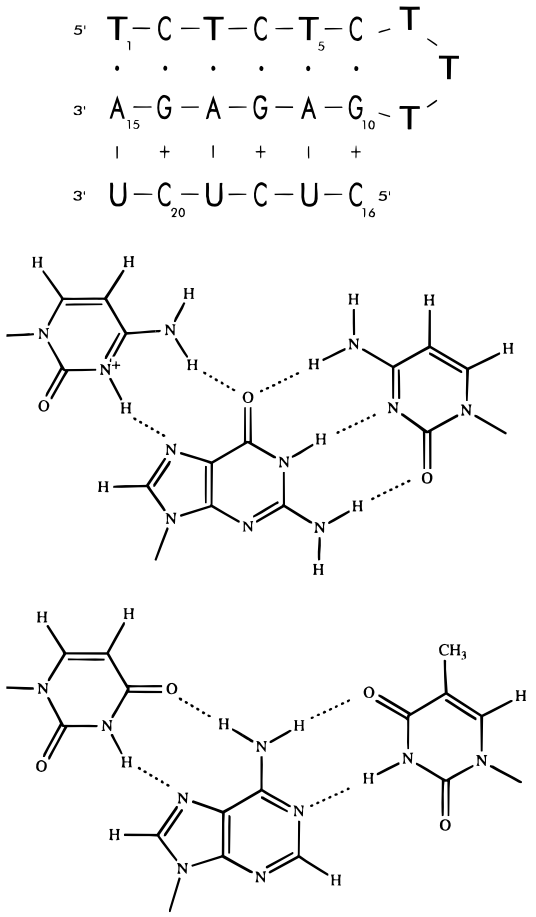

FIGURE 1: Nucleotide sequences and proposed folding and interaction of the DNA hairpin and the RNA oligonucleotide, with the subscripts indicating the residue numbering (top). Hydrogen bond schemes for the C·G*C$^+$ and T·A*U base triples involved (bottom).

resulted in self-consistent resonance assignments. However, if there is no such structural model available, a more general applicable method is required.

The approach followed in this study is the utilization of an unlabeled DNA hairpin and a uniformly $^{13}C/^{15}N$-enriched RNA oligonucleotide, making it possible to perform X-edited ^1H NMR spectroscopy (Otting et al., 1986; Bax & Weiss, 1986; Fesik et al., 1987; Otting & Wüthrich, 1989). By means of this type of experiment part of the spectrum can be filtered out, resulting in a reduction of spectral overlap, and even more importantly, intra- and interstrand cross peaks can be distinguished unambiguously. We report here on the application of improved versions of ^{15}N (ω_2) filtered NOESY and ^{13}C (ω_1) filtered NOESY experiments to the DNA−RNA complex dissolved in H_2O. The results give direct evidence for the formation of a triple helix between the DNA hairpin and the RNA oligonucleotide and also provide the essential features of its structure.

MATERIALS AND METHODS

Oligonucleotides. The DNA oligonucleotide 5′-TCTCTC-TTT-GAGAGA-3′ was synthesized on a Pharmacia LKB Geneassembler special, using the phosphotriester method (van Boom et al., 1983), and desalted by passing through G15 (Pharmacia).

The uniformly $^{13}C/^{15}N$-enriched RNA oligonucleotide 5′-CUCUCU-3′ was prepared by RNase T1 digestion of the RNA precursor 5′-pGGGAGCUCUCU-3′, which was synthesized by *in vitro* transcription of a partially duplex DNA template using T7-RNA polymerase (Milligan et al., 1987). The RNA precursor sequence was chosen such that it fulfills the promoter requirements of T7-RNA polymerase, which can only synthesize RNA oligos starting with guanosines. We chose GGGAG for the 5′-sequence, because in our experience this is one of the most efficient transcription starts for molecules of this size. Since the RNA target strand only contains pyrimidines, the undesired 5′-part can easily be removed by RNase T1, which specifically cleaves RNA at the 3′-side of guanosines, yielding 5′pGp3′, 5′Gp3′, 5′AGp3′, and 5′-CUCUCU-3′.

Synthesis and purification of the RNA precursor by polyacrylamide gel electrophoresis were as described in detail in Wijmenga et al. (1994). RNase T1 (Sigma) digestion was in 40 mM Tris-HCl, pH 7.6, at 37 °C, for 16 h, using 100 units of RNase T1/mg of RNA precursor. The RNase T1 digest was either purified by gel electrophoresis and subsequently desalted by gel filtration on TSK-HW40-TEAB (Omnilabo) followed by G10 (Pharmacia) or directly purified and desalted by gel filtration on G15 (Pharmacia). Final yields were approximately 2 mg from a 50 mL transcription reaction, using 1 mM $^{13}C/^{15}N$-enriched NTPs.

Sample Preparation. For the NMR sample 118 OD DNA was dissolved in 500 μL of 90% H_2O:10% D_2O, containing 0.1 M NaCl, and adjusted to pH 7.0 by addition of small amounts of HCl. Subsequently, a titration with the RNA was performed, until a DNA:RNA ratio of 1:1 was achieved, as judged from the relative intensities of the NMR signal of the aromatic protons. After this, the pH was gradually lowered to 5.0 by further addition of HCl, until the original imino proton spectrum was completely replaced by a new set of signals.

NMR Spectroscopy. One-dimensional ^1H spectra with GARP decoupling (Shaka et al., 1985) on ^{15}N and ^{13}C were recorded with the 1−1 spin echo sequence (Sklenář & Bax, 1987). Two different X-edited ^1H NMR spectra were acquired for the complex dissolved in H_2O, using the pulse sequences shown in Figure 2. These are modifications of the original sequences (Otting et al., 1986) to include suppression of the water signal without presaturation. In the sequence used to acquire the 2D ^{15}N (ω_2) filtered NOESY data, illustrated in Figure 2A, the 180° pulses on ^{15}N and ^{13}C served to refocus the heteronuclear $^1J_{NH}$ and $^1J_{CH}$ scalar couplings during t_1. To effect the suppression of the water signal in the ^{15}N (ω_2) filtered NOESY, a 1−1 spin echo sequence was built into the ω_2 filter. The ^1H 90° pulse after the NOE mixing period was replaced by a 90°−Δ−90° jump return sequence (Plateau & Guéron, 1982), and the ^1H 180° pulse in the filter period was replaced by a 90°−2Δ−90° sequence, similar to the way suppression of the H_2O signal is achieved in a HMQC sequence (Nikonowicz & Pardi, 1993). The delay Δ was set to $1/[4(\omega_{H_2O} - \omega_{NH})]$, resulting in a $\sin^3(\omega_{H_2O} - \omega)$ excitation profile, with a minimum at the H_2O resonance position and a maximum near the exchangeable proton resonances. The $90°_x - 90°_\psi$ editing pulses on ^{15}N were positioned in the middle of the 2Δ delay. The delay $\tau = 1/[2(^1J_{NH})]$ was set to 5.0 ms. GARP decoupling during detection was executed on both ^{15}N and ^{13}C. For optimal reduction of the H_2O signal, short homospoil delays were implemented during the relaxation delay and the NOE mixing period, respectively. An eight-step phase cycle was performed on $\phi_2-\phi_6$ to make the jump−

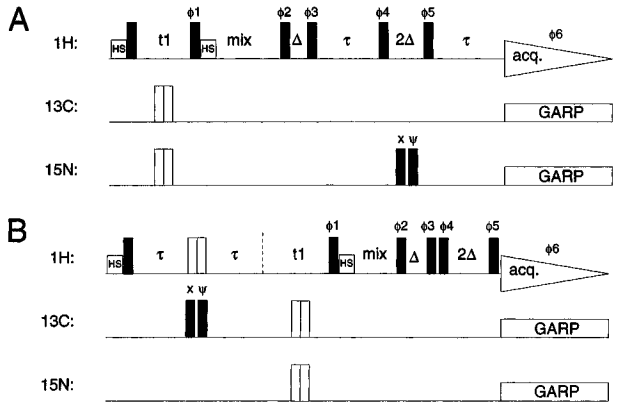

FIGURE 2: Pulse schemes of the ^{15}N (ω_2) filtered NOESY (A) and the ^{13}C (ω_1) filtered NOESY (B) experiments. The narrow filled bars represent 90°; the double open bars represent 180° pulses. Homospoil delays of 20 ms, which were applied during the relaxation delay and the NOE mixing period, are indicated by blocks marked with HS. Phase cycle for both experiments: $\phi_1 = 223°$; $\phi_2 = 4\ (x), 4\ (-x)$; $\phi_3 = 4\ (-x), 4\ (x)$; $\phi_4 = x, -x, y, -y, -x, x, -y, y$; $\phi_5 = -x, x, -y, y, x, -x, y, -y$; $\phi_6 = 2\ (x), 4\ (-x), 2\ (x)$. Nonlabeled pulses are parallel to the *x*-axis. Two separate data sets are acquired with $\psi = x$ and $\psi = -x$, respectively. To achieve phase-sensitive detection in the indirect dimension, the phase of the ^1H excitation pulse was alternately *x* and *y*, and the procedure was completed during processing by inverting the signs of every third and fourth data point. This approach allows the H_2O signal to be kept prior to acquisition for both the *x* and *y* phases of the ^1H excitation pulse in the $+z$ half of the *xyz* sphere, reducing radiation damping effects. In addition, keeping $(1/2)\sqrt{2}$ of the H_2O signal along the $+z$-axis prior to acquisition increases the signal intensity of the exchangeable protons (Kontaxis et al., 1994).

return−echo sequence selective against H_2O signals (Sklenář & Bax, 1987). The phase cycling was chosen such that $(1/2)\sqrt{2}$ of the H_2O signal lies along the $+z$-axis prior to acquisition. To reduce the residual water signal, the phase ϕ_1 was optimized to 223° with respect to the *x*-axis. Phase-sensitive detection of the indirectly observed frequency was achieved by a modification of the TPPI method (Marion & Wüthrich, 1983) and is further described in the caption of Figure 2. Two data sets were acquired in an interleaved manner and stored separately with $\psi = x$ and $\psi = -x$, respectively. The sequence for the ^{13}C (ω_1) filtered NOESY experiment (Figure 2B) differs from the previous one in the position of the filter only. The delay $\tau = 1/[2(^1J_{CH})]$ was set to 3.5 ms. We chose to apply two single half-filtered experiments, instead of one ^{13}C (ω_1)−^{15}N (ω_2) filtered NOESY experiment. Application of such a double-half-filtered experiment requires the duration time of the pulse sequence to be extended by a second filter delay of $1/[^1J_{XH}]$ (7−10 ms), thereby reducing the sensitivity of the the NOE cross peaks between the relatively fast exchangeable protons significantly. Both spectra were recorded at 600 MHz with 28.9 and 7.3 Hz resolution in f_1 and f_2, respectively, and with the NOE mixing period set to 400 ms. The temperature was 1 °C for the ^{15}N (ω_2) filtered NOESY and 13 °C for the ^{13}C (ω_1) filtered NOESY experiment.

Spectrum Processing. 1D spectra were processed with the nmr1 program of the NMRi software package (New Methods Research, Inc., Syracuse, NY). For the 2D spectra the MNMR software package (PRONTO Software Development and Distribution, Copenhagen, Denmark) was used. The $\psi = x$ and $\psi = -x$ data sets of the X-filtered NOESY experiments were processed separately. They were subsequently combined with addition and substraction factors optimized to produce pure sum and difference spectra, respectively.

RESULTS AND DISCUSSION

Here we present the results of an NMR study aimed at the characterization of the structure of the complex formed by the DNA hairpin with sequence 5′-TCTCTC-TTT-GAGAGA-3′ and the single-stranded RNA oligonucleotide 5′-CUCUCU-3′ at acidic pH. We found that a triple helix is formed (Figure 1), with base triple geometries that can be described by Watson−Crick and Hoogsteen hydrogen bonds, and with the RNA oligonucleotide acting as the third strand.

To characterize this triple helix structure, interstrand NOE contacts, i.e., contacts which directly reflect the interactions between the DNA hairpin and the RNA oligonucleotide, are crucial. Special attention needs therefore to be paid to identify these NOEs and to differentiate them from intra-strand contacts. This requires that the various proton resonances are unambiguously assigned to either the DNA or the RNA strand, which was realized by the utilization of an unlabeled DNA hairpin and a uniformly $^{13}C/^{15}N$-enriched RNA oligonucleotide in combination with X-edited ^1H NMR spectroscopy. ^{15}N (ω_2) filtered NOESY and ^{13}C (ω_1) filtered NOESY experiments (pulse sequences shown in Figure 2) were applied to this system, dissolved in H_2O, which resulted in the spectra presented in Figures 3 and 4, respectively.

Figure 3 shows parts of the sum and difference spectra generated from the ^{15}N (ω_2) filtered NOESY experiment. Because signals arising from ^{15}N-coupled protons have opposite signs in the $\psi = x$ and $\psi = -x$ data sets, the sum spectrum (Figure 3A,B) shows NOE contacts from any proton in the complex (f_1 dimension) to non-^{15}N-bound protons only (f_2 dimension), whereas the NOEs from any proton in the complex to protons bound to ^{15}N are exclusively visible in the difference spectrum (Figure 3C,D). It is noted that this separation includes the diagonal peaks; i.e., non-^{15}N-bound protons exhibit diagonal peaks in the sum spectrum; the diagonal peaks in the difference spectrum belong to ^{15}N-bound protons. For a complex between nonlabeled DNA and ^{15}N-labeled RNA, this approach differentiates between the NOEs to the exchangeable protons of the DNA and to the exchangeable protons of the RNA in the complex. Consequently, Figure 3A,B displays cross peaks from any kind of proton in the complex to the exchangeable protons of the DNA only and not to those of the RNA fragment. Henceforth, these figures will therefore be referred to as "all-to-DNA spectra". The NOEs to the imino and amino protons of the ^{15}N-enriched RNA fragment are exclusively visible in panels C and D of Figure 3, respectively. They will be further denoted as "all-to-RNA spectra". An immediate advantage of the approach is manifested by the separation of the signals of the DNA imino proton of G10 and the RNA imino proton of U21, both resonating at 13.06 ppm (Figure 3A,C).

In Figure 4 parts of the sum and difference spectra obtained from the ^{13}C (ω_1) filtered NOESY data are shown. The sum spectra (Figure 4A,B) exclusively exhibit NOE contacts from protons not coupled to ^{13}C, including all exchangeable protons, (f_1 dimension) to any proton (f_2 dimension). The NOEs originating from ^{13}C-bound protons can be found in the difference spectrum (Figure 4C,D). The

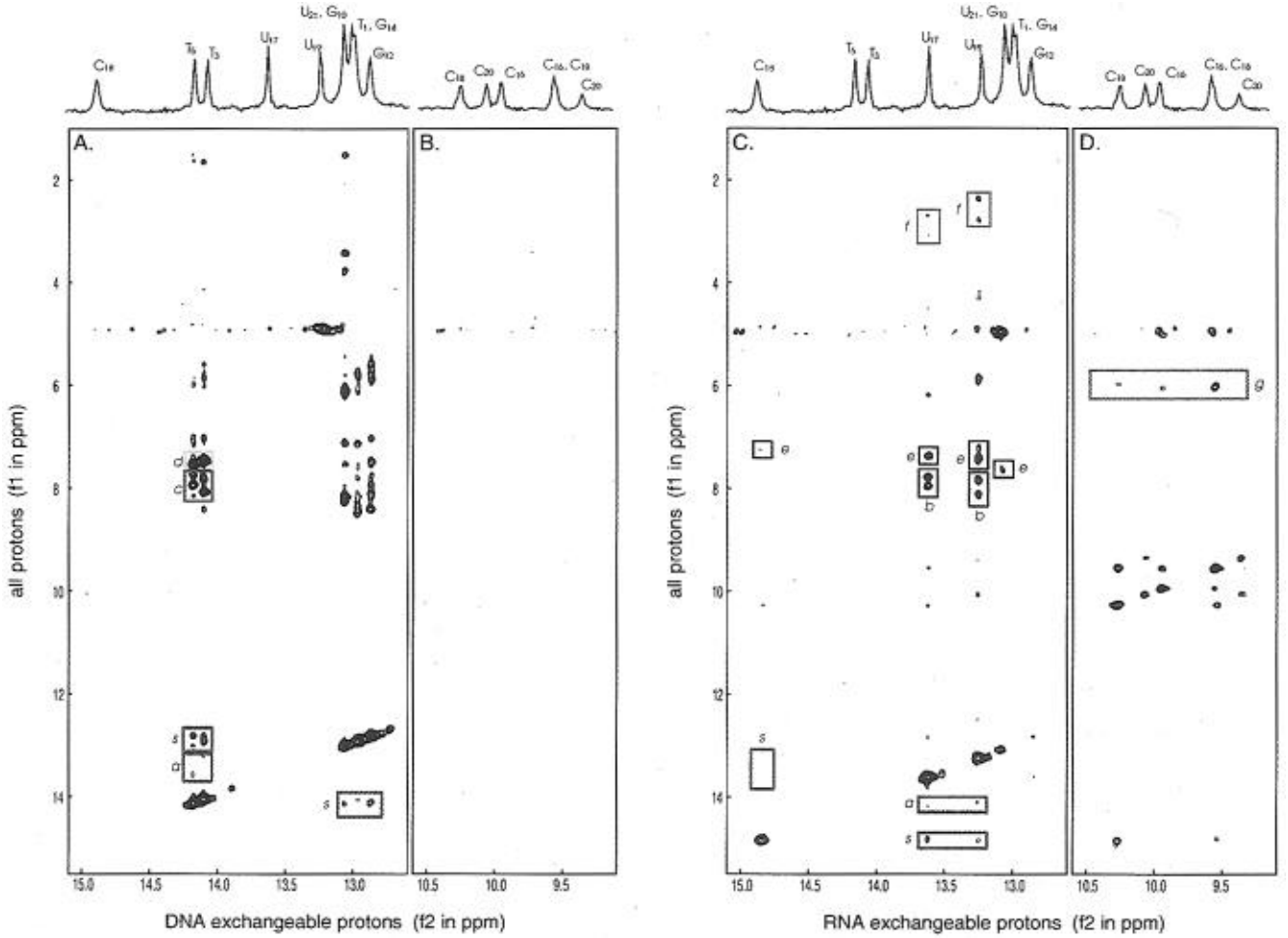

FIGURE 3: Parts of the spectrum obtained after summation (A, B) and subtraction (C, D) of the $\psi = x$ and $\psi = -x$ data sets from the ^{15}N (ω_2) filtered NOESY experiment. The sum spectrum shows NOEs to NH protons of the DNA (A), whereas in the difference spectrum the NOEs to NH protons of the RNA (C) and NH_2 protons of the RNA (D) are observed. The counterpart of (D) in the sum spectrum, (B), does not show any cross peaks. Boxed peaks are discussed in the text.

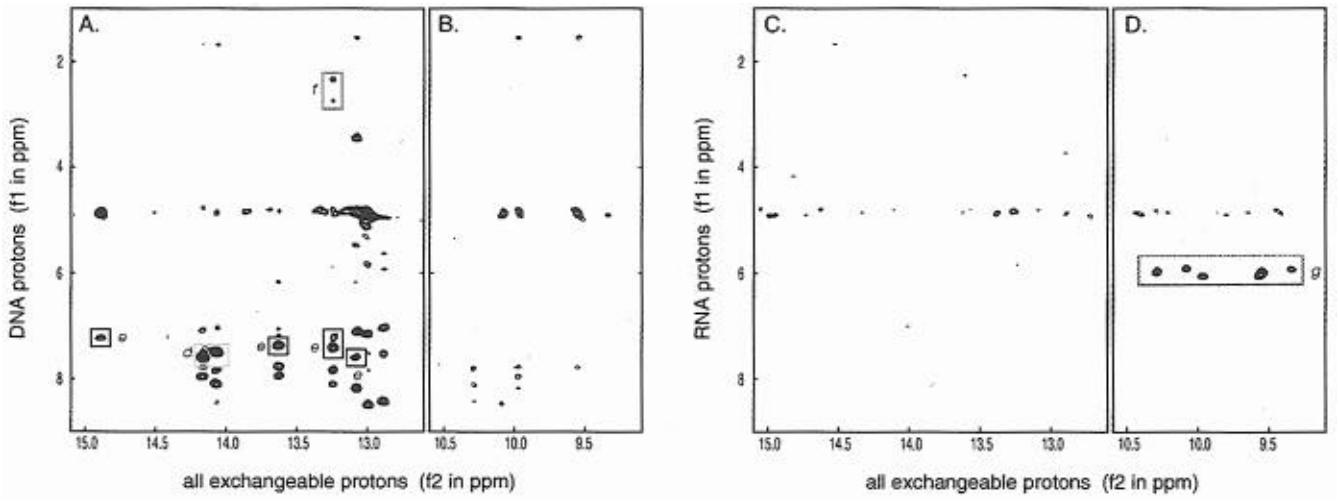

FIGURE 4: Parts of the sum (A, B) and difference (C, D) spectrum obtained from the ^{13}C (ω_1) filtered NOESY experiment. The sum spectrum shows NOEs from CH protons of the DNA and regularly shifted NH_2 protons to NH (A) and downfield-shifted NH_2 (B) protons. The difference spectrum shows NOEs from CH protons of the RNA to downfield-shifted NH_2 protons (B). The counterpart of (A) in the difference spectrum, (C), does not show any cross peaks. Boxed peaks are discussed in the text.

f_1 region in Figure 4 has been chosen such that, in addition to the carbon-bound protons of the complex, only DNA exchangeable amino protons are visible. Hence, in Figure 4A,B cross peaks from protons of the DNA strand are observed ("all-from-DNA spectra"), while Figure 4C,D exclusively shows cross peaks resulting from nonexchangeable protons of the RNA strand to all exchangeable protons of the complex ("all-from-RNA spectra").

The clear distinction that can be made between $^{13}C/^{15}N$-bound RNA protons and $^{12}C/^{14}N$-bound DNA protons allows unambiguous conclusions regarding the origin of the cross peaks, i.e., whether they stem from interstrand or from

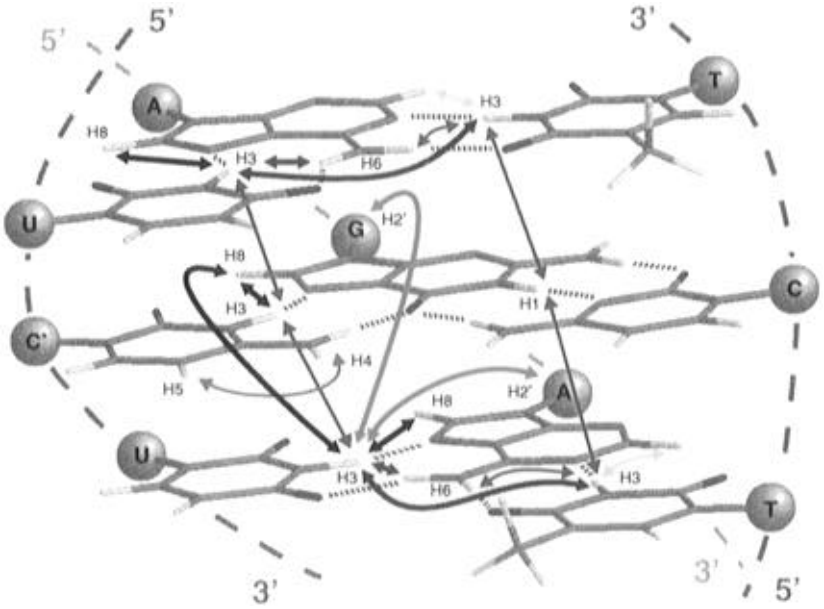

FIGURE 5: Schematic representation of the central part of the triple helix stem, with the intra- and interstrand contacts described in the text designated as thin and thick arrows, respectively. The colors of the arrows correspond to the colors of the boxes in Figures 3 and 4. The spheres connected by broken lines represent the sugar−phosphate backbones and indicate the orientation of the three strands with respect to each other.

intrastrand NOEs. The observation of a pair of cross peaks which are symmetrically situated with respect to the diagonal and connecting two diagonal peaks reveals an intrastrand DNA−DNA or RNA−RNA contact. An interstrand DNA−RNA contact, on the other hand, appears as a single cross peak at only one side of the diagonal and is connected to only one diagonal peak. For instance, the sum (all-to-DNA) spectrum of the ^{15}N (ω_2) filtered experiment shows pairs of imino−imino cross peaks, indicated by the boxes marked with *s* (Figure 3A), which correspond to the sequential contacts between consecutive base pairs in the DNA molecule, expected for a helix with Watson−Crick base pairs. The difference (all-to-RNA) spectrum shows cross peak pairs symmetrically situated between imino proton resonances of the RNA strand, also indicated by boxes marked with *s* (Figure 3C). Although one of the resonances is seriously broadened by solvent exchange, resulting in the apparent absence of the cross peak above the diagonal, the observation of both diagonal peaks still allows this unambiguous classification. The pronounced downfield shift of the involved imino proton resonance at 14.84 ppm, as well as its NOE contacts to ^{15}N-coupled amino protons resonating in the characteristic region between 9.0 and 10.5 ppm (see Figure 3D), reveals that this imino proton belongs to a protonated cytosine residue. It shows NOE contacts to the imino protons of two neighboring uracil residues. The intrastrand DNA−DNA and RNA−RNA NOE contacts were used to obtain structure-independent sequence-specific resonance assignments for the exchangeable as well as some nonexchangeable protons of both strands (see Figure 3).

As stated above, an interstrand NOE contact is seen as a single cross peak at one side of the diagonal, connected to only one diagonal peak, in the sum as well as in the difference spectrum. For the DNA−RNA complex these asymmetrically situated cross peaks are, for instance, observed between the imino proton resonances of thymine and uracil bases in the ^{15}N (ω_2) filtered experiment. They are indicated in Figure 3A,C by boxes marked with *a*. The obtained sequence-specific assignments demonstrate that these NOEs occur within the T·A*U base triples and that they are build up through spin diffusion via the amino protons of the shared adenine residue (*vide infra*).

Further inspection of the entire spectra (additional regions not shown) establishes that the cross peaks marked with *b* are interstrand contacts as well. They are attributed to NOEs between adenine amino protons of the DNA strand and RNA imino protons of uracil residues. The cross peaks marked with *c* are NOEs within the DNA stem between the same adenine amino protons and the thymine imino protons. Together they constitute the spin diffusion pathway necessary to bring about the interstrand imino−imino cross peaks mentioned above (boxes *a*).

The ^{15}N (ω_2) filtered NOESY spectrum alone is not sufficient for an unambiguous assignment of the aromatic ring and sugar proton resonances in the f_1 dimension to either DNA or RNA, because these protons are attached to carbon rather than nitrogen (boxes *d* in Figure 3A, *e* and *f* in Figure 3C, and *g* in Figure 3D). The ^{13}C (ω_1) filtered NOESY spectrum resolves this ambiguity. The cross peaks marked *d* in the all-to-DNA spectrum (Figure 3A) return in the all-from-DNA spectrum (Figure 4A) and not in the all-from-RNA spectrum (Figure 4C), which demonstrates that they correspond to contacts within the DNA strand. Analogously, the cross peaks marked *e* are attributed to interstrand DNA−RNA contacts. Further analysis revealed that these NOE contacts originate from H2 protons of adenine residues (*d*) and H8 protons of the purine strand (*e*) of the DNA, respectively. In the same manner it could be deduced that the cross peaks marked with *f* in Figure 4A correspond to interstrand contacts between imino protons of uracil residues in the RNA strand and H2′/H2″ protons of purine residues in the DNA strand. This conclusion is corroborated by the characteristic upfield chemical shift of the latter protons. For the cross peaks in the region of the ^{15}N (ω_2) filtered NOESY spectrum where NOEs between H5/H1′ and amino protons of protonated cytosines are expected to be observed (Figure 3D, boxes *g*), the presence of these NOEs in the all-from-RNA spectrum (Figure 4D) and absence in the all-from-DNA

spectrum (Figure 4B) definitely establish that the resonances in the f_1 dimension can be attributed to RNA protons and therefore that the cross peaks involved are intraresidue NOEs. Additional information established that they are H5−amino proton contacts within the protonated cytosine residues.

Combining the sequence-specifically assigned inter- and intrastrand NOE contacts clearly demonstrates the formation of a triple helix structure, which involves a DNA hairpin with a stem to which an RNA oligonucleotide is bound. Figure 5 indicates the various contacts described above in a schematic representation of the three-dimensional structure of the central part of the triple helix stem. As can be gleaned from this figure, two separate pathways of sequential imino−imino NOEs are observed. The first one links the DNA imino protons involved in hydrogen bonds, whereas the second one does this for the hydrogen-bonded imino protons of the RNA strand. These two pathways are connected to each other by cross-strand contacts. First, the connectivities from the thymine imino protons via adenine amino to uracil imino protons, supported by the aforementioned spin diffusion contacts, position the RNA strand in a parallel orientation relative to the purine strand. Additional cross-strand contacts between DNA H8 and RNA imino protons and between DNA amino and RNA imino protons localize the RNA strand in the major groove of the Watson−Crick helix, in such a way that Hoogsteen-type hydrogen bonds can be formed. Furthermore, sequential contacts (5′ to 3′) from H8 (and also H2′/H2″) of the purine residues of the DNA strand to imino protons of the RNA strand unambiguously show that the helix has a right-handed configuration. NOEs between Hoogsteen base-paired imino protons and H2′ and H2" protons from the 5′-neighboring purine base were earlier observed and recognized as excellent indicators of triple helix formation (Macaya et al., 1992), based on the available X-ray fiber diffraction data for all-DNA triple helices.

Unlike the structure determination studies performed for all-DNA triple helices, in this study we could not rely on an initial structural model, since no X-ray data are available for a triple helix with strands composed of both DNA and RNA. Nevertheless, we were able to structurally characterize the complex and in this way diminish the uncertainties of such hybrid triple helix structures depicted by Frank-Kamenetskii and Mirkin (1995). We found that the RNA strand is bound in the major groove of the Watson−Crick stem of the DNA hairpin by the formation of Hoogsteen hydrogen bonds and is oriented in a parallel fashion with respect to the purine strand of this hairpin. The thus formed DNA−RNA triple helix is right-handed. These features very much resemble those of the intramolecular triple helix structures of all-DNA systems (Macaya et al., 1992; Radhakrishan & Patel, 1994a,b) in spite of the incorporation of an RNA strand. The formation of an alternative triple helix structure formed from two identical DNA strands, as described by Mooren et al. (1990), could be ruled out as a result of the unambiguous discrimination between the DNA and RNA strands. Interstrand DNA−DNA contacts, which would disclose such a structure, were not observed in the spectra. Apparently, the presence of the RNA strand prevents this structure from being formed, revealing the higher stability of the DNA−RNA complex.

In conclusion, the structure of the triple helix formed by the DNA hairpin 5′-TCTCTC-TTT-GAGAGA-3′ and the single-stranded RNA oligonucleotide 5′-CUCUCU-3′ at acidic pH was characterized by the combined application of ^{15}N (ω_2) and ^{13}C (ω_1) filtered NOESY experiments. This approach proves to be excellent for the discrimination between intra- and interstrand NOE contacts, which is a crucial step in the structure determination of bimolecular systems. It permits sequence-specific assignments of the exchangeable and some nonexchangeable protons to be performed and structure information of the "isolated" strands, supplemented by specific cross-strand contacts, defining the relative orientation of the two molecules to be derived. Moreover, the separation of the cross peaks into two subspectra reduces spectral overlap, which allows for its application to larger systems.

ACKNOWLEDGMENT

NMR spectra were recorded at the Dutch National hf-NMR Facility (Nijmegen, The Netherlands) supported by SON. We wish to thank J. Joordens for excellent technical assistance.

REFERENCES

Bax, A., & Weiss, M. A. (1986) *J. Magn. Reson. 71*, 571−575.
Burkholder, G. D., Latimer, L. J. P., & Lee, J. S. (1988) *Chromosoma 97*, 185−192.
Burkholder, G. D., Latimer, L. J. P., & Lee, J. S. (1991) *Chromosoma 101*, 11−18.
de los Santos, C., Rosen, M., & Patel, D. J. (1989) *Biochemistry 28*, 7282−7289.
Escudé, C., François, J.-C., Sun, J.-s., Ott, G., Sprinzl, M., Garestier, T., & Hélène, C. (1993) *Nucleic Acids Res. 21*, 5547−5553.
Fesik, S. W., Gampe, R. T., Jr. & Rockway, T. W. (1987) *J. Magn. Reson. 74*, 366−371.
François, J.-C., Saison-Behmoras, T., Thuong, N. T., & Hélène, C. (1989) *Biochemistry 28*, 9617−9619.
Frank-Kamenetskii, M. D., & Mirkin, S. M. (1995) *Annu. Rev. Biochem. 64*, 65−95.
Hampel, K. J., Ashley, C., & Lee, J. S. (1994) *Biochemistry 33*, 5674−5681.
Han, H., & Dervan, P. B. (1993) *Proc. Natl. Acad. Sci. U.S.A. 90*, 3806−3810.
Horne, D. A., & Dervan, P. B. (1990) *J. Am. Chem. Soc. 112*, 2435−2437.
Ing, N. H., Beekman, J. M., Kessler, D. J., Murphy, M., Jayaraman, K., Zendegui, J. G. Hogan, M. E., O'Malley, B. W., & Tsaj, M.-J. (1993) *Nucleic Acids Res. 21*, 2789−2796.
Kontaxis, G., Stonehouse, J., Laue, E. D., & Keeler, J. (1994) *J. Magn. Reson. A 111*, 70−76.
Lee, J. S., Latimer, L. J. P., Haug, B. L., Pulleyblank, D. E., Skinner, D. M., & Burkholder, G. D. (1989) *Gene 82*, 191−199.
Macaya, R., Wang, E., Schultze, P., Sklenář, V., & Feigon, J. (1992) *J. Mol. Biol. 225*, 755−773.
Marion, D., & Wüthrich, K. (1983) *Biochem. Biophys. Res. Commun. 113*, 967−974.
Milligan, J. F., Groebe, D. R., Witherell, G. W., & Uhlenbeck, O. C. (1987) *Nucleic Acids Res. 15*, 8783−8798.
Mooren, M. M. W., Pulleyblank, D. E., Wijmenga, S. S., Blommers, M. J. J., & Hilbers, C. W. (1990) *Nucleic Acids Res. 18*, 6523−6529.
Nikonowicz, E. P., & Pardi, A. (1993) *J. Mol. Biol. 232*, 1141−1156.
Otting, G., & Wüthrich, K. (1989) *J. Magn. Reson. 85*, 586−594.
Otting, G., Senn, H., Wagner, G., & Wüthrich, K. (1986) *J. Magn. Reson. 70*, 500−505.
Plateau, P., & Guéron, M. (1982) *J. Am. Chem. Soc. 104*, 7310−7311.
Pvosic, T. J., & Dervan, P. B. (1990) *J. Am. Chem. Soc. 112*, 9428−9430.
Radhakrishnan, I., & Patel, D. (1993) *Structure 1*, 135−152.
Radhakrishnan, I., & Patel, D. (1994a) *Structure 2*, 17−32.

Radhakrishnan, I., & Patel, D. (1994b) *J. Mol. Biol. 241*, 600−619.
Rajagopal, P., & Feigon, J. (1989) *Nature 339*, 637−640.
Roberts, R. W., & Crothers, D. M. (1992) *Science 258*, 1463−1465.
Roy, C. (1993) *Nucleic Acids Res. 21*, 2845−2852.
Shaka, A. J., Barker, P., & Freeman, F. (1985) *J. Magn. Reson. 64*, 547−552.
Sklenář, V., & Bax, A. (1987) *J. Magn. Reson. 74*, 469−479.
Sklenář, V., & Feigon, J. (1990) *Nature 345*, 836−838.
Skoog, J. U., & Maher, L. J. (1993) *Nucleic Acids Res. 21*, 2131−2138.
Ulrich, M. J., Gray, W. J., & Ley, T. J. (1992) *J. Biol. Chem. 267*, 18649−18658.
van Boom, J. H., van der Marel, G. A., Westerink, H. P., van Boeckel, C. A. A., Mellema, J. R., Altona, C., Hilbers, S. W., Haasnoot, C. A. G., de Bruin, S. H., & Berendsen, R. G. (1983) *Cold Spring Harbor Symp. Quant. Biol. 47*, 403−409.
Wijmenga, S. S., Heus, H. A., van de Ven, F. J. M., & Hilbers, C. W. (1994) in *NMR of Biological Macromolecules* (Stassinopoulou, C. I., Ed.) Nato ASI Series, Vol. 87, pp 307−322, Springer, Berlin, Germany.

BI952002F